Sources and Fate of Sedimentary Organic Matter in the Western Mediterranean Sea

Journal Article

Author(s):
Ausín, Blanca; Bossert, Gina; Krake, Nicola; Paradis, Sarah (iD); Haghipour, Negar; de Madron, Xavier Durrieu; Alonso, Belen; Eglinton, Timothy

Key Points:

- Geochemical and sedimentological signals depict a clear SW-NE gradient that reverses in the Gulf of Lions
- This gradient is mainly attributed to differences in local primary productivity and delivery of terrestrial organic carbon
- Organic matter protection by mineral surfaces and lateral transport are proposed as potential additional controls

Author Contributions:

Conceptualization: Blanca Ausín, Timothy Eglinton
Data curation: Blanca Ausín, Gina Bossert
Formal analysis: Blanca Ausín, Gina Bossert, Nicola Krake, Sarah Paradis, Negar Haghipour
Funding acquisition: Blanca Ausín, Timothy Eglinton
Investigation: Blanca Ausín, Gina Bossert, Nicola Krake, Timothy Eglinton

Sources and Fate of Sedimentary Organic Matter in the Western Mediterranean Sea

Blanca Ausín[1,2] ![ORCID], Gina Bossert[2], Nicola Krake[2,3], Sarah Paradis[2] ![ORCID], Negar Haghipour[2] ![ORCID], Xavier Durrieu de Madron[4] ![ORCID], Belén Alonso[5], and Timothy Eglinton[2]

[1]Universidad de Salamanca, Salamanca, Spain, [2]ETH Zurich, Zurich, Switzerland, [3]University of Hamburg, Hamburg, Germany, [4]French National Centre for Scientific Research (CEFREM), Perpignan, France, [5]Instituto de Ciencias del Mar (ICM-CSIC), Barcelona, Spain

Abstract Marine sediments comprise the primary long-term sink of organic matter (OM) in marine systems. Disentangling the diverse origins of OM and the influence of the main processes that determine organic carbon (OC) fate at a global scale has proven difficult due to limited spatial data coverage. Thus, comprehensive studies of the spatial distribution of the content and geochemical characteristics of sedimentary OM at basin scales provide fundamental knowledge on the role of marine sediments in the global carbon cycle. Here, we shed light on the origin of OM and the underlying mechanisms that determine its fate in a semi-enclosed basin by examining the spatial patterns in the isotopic and elemental composition of OM in 149 core-top samples from the Western Mediterranean Sea and the adjacent Atlantic Ocean sector. Our results reveal an apparent SW-NE gradient that reverses in the Gulf of Lions in most geochemical and sedimentological features. Changes in the OC content and δ^{13}C and Δ^{14}C signatures are ascribed to spatial variations in marine primary productivity and the influence of varying discharge of rivers and well-developed canyons that favor the cross-shelf transport of terrestrial (and petrogenic) OC. Our results also suggest the potential influence of two other mechanisms on the geochemical signatures of OM: (a) lateral transport of allochthonous OC and selective degradation of labile OM, which potentially occurs across the studied area having a greater impact toward the north-eastern region, and (b) OM protection via association with mineral surfaces, potentially having a greater influence toward the south-western basins.

1. Introduction

Marine sediments are one of the largest global carbon sinks, with continental margins acting as key areas of organic carbon (OC) storage (Atwood et al., 2020; Hedges & Keil, 1995). Understanding the factors and processes that determine the stabilization of organic matter (OM) on continental margins and their adjacent deep oceanic domain is vital to constrain global carbon inventories and carbon cycling. Sedimentary OM is composed of varying proportions of marine and terrestrial OC. Each of these pools may, in turn, combine with freshly produced OC from primary productivity, aged and altered OC that has been retained in the system prior to final burial, and fossil or rock-derived (petrogenic) OC mainly introduced by fluvial transport. Isotopic (δ^{13}C, δ^{15}N, and Δ^{14}C) and elemental (carbon and nitrogen content and atomic C/N ratios) characteristics of sedimentary OM allow to identify contrasting combinations of these three components on the basis of their primary origin and reactivity (Meyers, 1994).

Once in the water column, OM is transformed and degraded by chemical, physical and biological processes (Burdige, 2007), with exposure to oxic conditions playing a major role in favoring OM remineralization. Protection from oxic degradation is promoted via organo-mineral associations (Hemingway et al., 2019; Mayer, 1994a, 1994b). OM sorption onto particle surfaces is greater in finer grains because the latter provide a higher surface area to volume ratio. Accordingly, there is a broadly linear relationship between OC content and mineral surface area (SA), which is in turn inversely related to grain size. However, fine-grained minerals may further expose hosted OM to transport under oxic conditions because non-cohesive fine-grained sediments (i.e., silt; 2–63 μm) are more prone to resuspension and subsequent lateral advection than cohesive fine grains (i.e., clay; <2 μm) and coarser grains (i.e., sand; >63 μm) (Ausín et al., 2021). Hence, the hydrodynamic sorting of fine-grained sediment favors OC degradation (Blair & Aller, 2012). Since hydrodynamic processes play a crucial role in the dispersal and characteristics of sedimentary OM (Ausín et al., 2021; Bao et al., 2018; Bröder

Methodology: Blanca Ausín, Sarah Paradis

Project Administration: Blanca Ausín, Timothy Eglinton

Resources: Xavier Durrieu de Madron, Belén Alonso, Timothy Eglinton

Supervision: Blanca Ausín, Timothy Eglinton

Visualization: Blanca Ausín, Gina Bossert

Writing – original draft: Blanca Ausín, Gina Bossert

Writing – review & editing: Sarah Paradis, Negar Haghipour, Xavier Durrieu de Madron, Belén Alonso, Timothy Eglinton

et al., 2018; Bruni et al., 2022), the distribution and geochemical composition of OM must also be assessed in a sedimentological context.

Integrated studies on the origin and fate of sedimentary OC at basin scales are limited because it is difficult to disentangle the various biological, physico-chemical, and geological processes that influence the geochemical and sedimentological characteristics of OM. Yet, a comprehensive assessment of the influence of these processes at basin scales is vital in understanding the role of marine sediments in the global carbon cycle.

In this regard, spatially restricted seas provide a natural laboratory to assess in detail the diverse OM origins and varied depositional processes that influence the spatial distribution of the content and geochemical characteristics of sedimentary OM.

Here, we examine the spatial distribution of the content and geochemical characteristics of sedimentary OM in surface sediment samples from the Atlantic sector west of the Strait of Gibraltar and across the Western Mediterranean Sea to improve our understanding of carbon cycling on continental margins and adjacent deep basins and shed light on the underlying processes that might impact OM signals in the sedimentary record and their interpretation in paleoenvironmental studies.

2. Study Area

The Western Mediterranean Sea (Figure 1) is a semi-enclosed basin whose restricted connection to the open ocean allows examination of the major processes that control the distribution and geochemical characteristics of sedimentary OM on continental margins and in neighboring deeper environments. In this work, the Western Mediterranean has been divided into smaller basins following Bricaud et al. (2002): Alboran Sea, Algerian Basin, Balearic Sea, Algero-Provencal Basin, and Gulf of Lions. Because the Atlantic water enters the Mediterranean Sea through the Strait of Gibraltar and mixes with the more saline, warmer, and oligotrophic Mediterranean water, influencing the resulting geochemical signature of Mediterranean surface waters, the adjacent Atlantic sector (SW Iberian margin) west of the Strait of Gibraltar is also included in this study.

The SW Iberian margin is part of the Canary Current Upwelling System and is characterized by strong mesoscale gradients and seasonal variability in upwelling occurrence and primary productivity (Relvas et al., 2007). The Western Mediterranean Sea is considered mesotrophic with annual mean values of net primary production of 131 ± 6 g C m^{-2} yr^{-1} (Lazzari et al., 2012) due to wind-induced winter mixing and coastal upwelling (Siokou-Frangou et al., 2010). The annual primary production is relatively high in the Alboran Sea (215–244 gC m^{-2} yr^{-1} (Bosc et al., 2004)) due to the presence of upwelling cells related to semi-permanent geostrophic fronts associated with the inflow of Atlantic waters (Sarhan et al., 2000). The annual primary production decreases toward the northeast throughout the Algerian Basin, the Balearic Sea, and the Algero-Provencal Basin (158–156, 153–175, and 145–165 gC m^{-2} yr^{-1}, respectively (Bosc et al., 2004)). Values are higher in the Gulf of Lions (180–204 gC m^{-2} yr^{-1}) due to intense convective mixing in winter, which causes a large planktonic bloom in spring (Kessouri et al., 2018; Mayot et al., 2017).

Large rivers are absent along the Portuguese coast south of Lisbon, whereas the Guadiana and Guadalquivir rivers discharge water at annual mean rates of 180 m^3 s^{-1} and 230 m^3 s^{-1} on average, respectively, into the Gulf of Cadiz, which connects surface-flowing North Atlantic waters with the Mediterranean waters flowing at depth (Figure 1). To the east, the annual mean river discharge of each minor European and African river ranges between 5 and 50 m^3 s^{-1} to the Alboran Sea (Struglia et al., 2004). The annual mean fluvial discharge across the Western Mediterranean catchment area increases toward the northeast, with African rivers contributing each between 5 and 150 m^3 s^{-1} to the Algerian Basin and major annual mean contributions from the Ebro River (300–500 m^3 s^{-1}) and the Rhone River (1,500–1,800 m^3 s^{-1}) draining into the Balearic Sea and the Gulf of Lions, respectively (Figure 1) (Struglia et al., 2004). Like most rivers with large drainage basins (Blair & Aller, 2012), the Ebro and the Rhone rivers transport and deliver large amounts of pre-aged and petrogenic terrestrial OC eroded from sedimentary rock outcrops, which for these rivers are mainly composed of sandstone, limestone and shales (Ollivier et al., 2010; Soria-Jáuregui et al., 2019). Offshore sediment dispersal from the Ebro River is limited to the broad continental shelf of the Balearic Sea (Arnau et al., 2015), whereas sediments delivered by the Rhone River might be intercepted by canyons and transported to the deeper basin of the Gulf of Lions and along the continental margin of the Balearic Sea (Palanques et al., 2006).
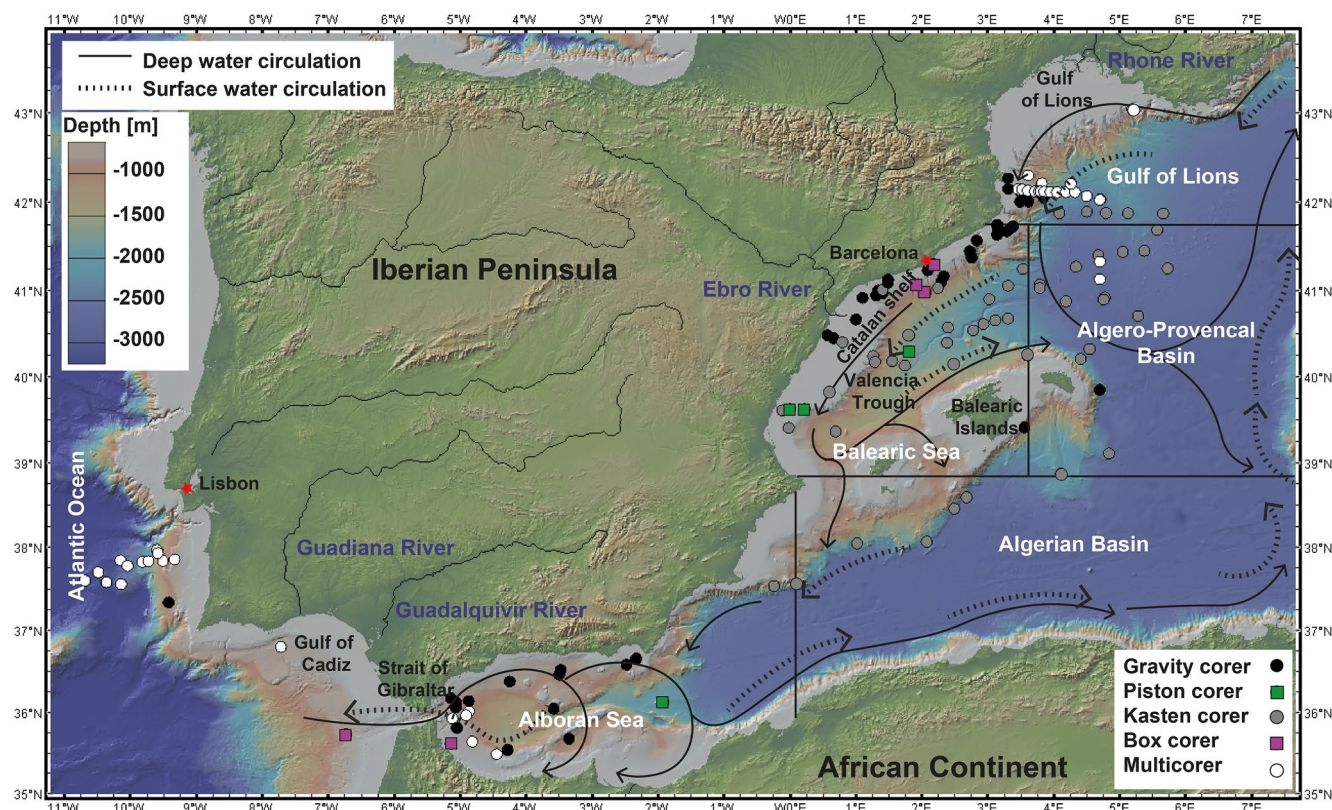
Figure 1. Study area and location of the 149 surface sediment samples. Surface and deep water circulation is marked by solid and dashed arrows, respectively. Colored symbols indicate sampling location and coring device used. The Mediterranean Sea is divided into smaller basins following Bricaud et al. (2002).

Previous studies have addressed the influence of other local-scale processes and features on the fate of OM in this region. For instance, lateral transport of fine-grained sediments via intermediate and bottom nepheloid layers has been suggested to contribute to the dispersal and geochemical signature of OC in the SW Iberian margin (Magill et al., 2018). Submarine canyons incising the European margin play a major role channeling sediments resuspended from the shelf toward the deeper basins. The most prominent canyon in the south-western basins is the Almeria Canyon, affected by active tectonics and characterized using downslope processes (García et al., 2006). Yet, canyons are more abundant and developed toward the northeast (Canals et al., 2013) where they channel shelf sediments resuspended by storms and coastal processes (e.g., wave activity and local outfalls) basinward (Quirós-Collazos et al., 2017), leading to the preferential off-shelf export of fine-grained sediments enriched in OC (Pedrosa-Pàmies et al., 2013). Sediments are drained by canyons to the deep basin by sediment gravity flows. The latter mainly include turbidity currents, as observed in the Valencia Trough (Amblas et al., 2011; O'Connell et al., 1985), but also dense shelf water cascading, as in the Gulf of Lions (Durrieu de Madron et al., 2023). Here, intense winter storms coupled with the overflow of cold, dense-shelf waters that are channeled through submarine canyons, drive large volumes of eroded sediment and aged OC toward the deep-sea (Canals et al., 2006; Tesi et al., 2010), although the OC signal of these events on the slope is masked by the intrinsic heterogeneity of surface sediments (Durrieu de Madron et al., 2020).

Finally, the bottom trawling activity performed on the margin down to 1,000 m depth is also responsible for grain size sorting and modifies OM composition (Paradis, Goñi, et al., 2021). Such activity triggers sediment gravity flows into submarine canyons (Puig et al., 2012) that may form persistent nepheloid layers (Arjona-Camas et al., 2021) that also affect the OM signature that is transported toward the deep sea (Paradis et al., 2022).

3. Methods

3.1. Sample Description

A total of 149 core-top samples were analyzed: 134 from the Western Mediterranean Sea and 15 from the adjacent Atlantic Ocean, west of the Strait of Gibraltar (Figure 1 and Table S1 in Supporting Information S1). The

samples were retrieved at water depths ranging from 18 to 4,672 m during several oceanographic cruises carried out between 1979 and 2011 using a variety of coring devices (gravity corer, piston corer, kasten corer, box corer, and multicorer). Multicore and box core samples were sliced onboard at 0.5 or 1 cm and kept at 4°C until the return to the laboratory. Sediment cores, on the other hand, were stored at the Core Repository of the Institute of Marine Sciences (CSIC) in Barcelona until sampling of the top cm (0–1 cm) for this investigation. All sediments were stored at −20°C in different laboratories and freeze-dried prior to analyses.

3.2. Radiocarbon Analyses

Samples analyzed for radiocarbon ($^{14}C/^{12}C$) were measured as CO_2 gas in a Mini Carbon Dating System (MICADAS) with a gas ion source at the Laboratory of Ion Beam Physics, ETH Zürich.

For OC-^{14}C analyses, between 20 and 25 mg of freeze-dried and homogenized sediment were fumigated in silver capsules with concentrated HCl (37%, 72 hr) to remove inorganic carbon and subsequently neutralized under a basic atmosphere (NaOH pellets, 72 hr) in a desiccator at 60°C. Samples were wrapped in tin capsules and OC-^{14}C was determined by Elemental Analyzer–Accelerator Mass Spectrometry (EA–AMS). Processing blanks, consisting of fossil (in-house shale) and modern (in-house sediment) reference materials were prepared following the same procedure. The oxalic acid reference material (NIST SRM 4990C) was used as a normalization standard. The method proposed by Welte et al. (2018) was adopted to assess and correct for capsule contribution and constant contamination introduced during sample fumigation and EA–AMS measurements. The estimated correction parameters were a carbon mass of 6.3 ± 1.6 µg with a F^{14}C of 0.65 ± 0.19. These values are higher than the long-term mean of the ETH laboratory (2–3 µg C). The source of contamination was not investigated; nevertheless, all the samples were prepared as large samples (>100 µg C), the subsequent correction did not substantially modify the F^{14}C values, and the error associated with the corrected values is <2% for most samples.

Planktic foraminifera-^{14}C was used as an indication of the age of surface sediments. Unlike OC bound to fine minerals, planktic foraminifera are large and dense, and thus less prone to resuspension and redistribution. Approximately 3 g of freeze-dried sediment from 27 samples were wet-sieved with tap water through 63- and 150-µm mesh sieves and thoroughly washed with deionized water prior to drying at 60°C overnight. Well-preserved tests of *Globigerina bulloides*, *Neogloboquadrina incompta*, or *Globorotalia inflata* were collected to determine ^{14}C from 40 to 100 µg of C using an automated method for acid digestion of carbonates (Wacker et al., 2013). ^{14}C determinations were corrected for isotopic fractionation via $^{13}C/^{12}C$ isotopic ratios.

^{14}C data for OC and foraminifera are reported here in $\Delta^{14}C$ notation (Stuiver & Polach, 1977).

3.3. ^{210}Pb Analyses

Only a subset of 29 samples had sufficient material for excess ^{210}Pb analyses, which was used to determine the recent (<∼100 years) deposition of sediment in core-tops following Sánchez-Cabeza et al. (1998) at the Autonomous University of Barcelona. Briefly, 200–300 mg of homogenized sediment was microwave-digested using concentrated HF, HNO_3, and HBO_3, using ^{209}Po as an internal tracer. The resulting solutions were evaporated and reconditioned with 1 M HCl. Polonium isotopes were spontaneously deposited onto silver disks while stirring at 70°C for 8 hr. Alpha emissions of ^{209}Po (4,883 keV) and ^{210}Po (5,304 keV) were quantified using passivated implanted planar silicon (PIPS) detectors (CANBERRA, model PD-450.18 a.m.) and the Genie™ data acquisition software. Concentrations of ^{210}Po were then transformed into total ^{210}Pb concentrations assuming secular equilibrium of both radionuclides at the time of analysis. Excess ^{210}Pb concentrations were obtained by subtracting total ^{210}Pb from supported ^{210}Pb concentrations, the latter obtained from data of sediment cores in the area (Martín et al., 2014; Masqué et al., 2002; Paradis et al., 2018).

3.4. Stable Isotopic and Elemental Analyses of OM

Organic carbon content (dry weight; OC$_\%$) was measured simultaneously with OC-^{14}C on the same aliquots by EA–AMS (Section 3.2) to an accuracy of better than 0.1% based on standards.

Between 10 and 15 mg of freeze-dried and homogenized sediment were fumigated as described for OC$_\%$ and OC-^{14}C to determine stable carbon isotopic composition (δ^{13}C) on an EA coupled in continuous flow with a Delta

V isotope ratio mass spectrometer (EA-iRMS). Values are reported relative to the Vienna Pee Dee Belemnite and precision was better than 0.1 ‰ (1σ) based on replicate measurements of standards. For total nitrogen content ($N_\%$) and stable nitrogen isotopic composition ($\delta^{15}N$), approximately 30 mg of freeze-dried and non-decarbonated sediment were analyzed via EA-iRMS. $\delta^{15}N$ values are reported relative to N_2 in air. The atomic C/N ratio was then calculated using $N_\%$ and $OC_\%$.

3.5. Grain Size and Mineral SA

For grain-size and SA estimates, freeze-dried sediments were combusted (450°C, 12 hr) to remove OM and cooled down slowly (50°C per hour) prior to analyses.

Between 1 and 2 g of combusted sediment were suspended in a solution of sodium hexametaphosphate in Milli-Q® water (1 g L^{-1}) and analyzed via laser diffraction on a Mastersizer 2000. Samples were measured in triplicates under repeatable conditions. Results were analyzed in terms of clay (<2 μm), fine silt (2–10 μm), coarse silt (10–63 μm), and sand (>63 μm).

Between 150 and 500 μg of combusted sediment were used for the analyses of nitrogen-based BET (Brunauer–Emmett–Teller) surface area on a Quantachrome NOVA 4000e. Degassing was performed using a Quantachrome FLOVAC degasser at 350∘C for 2 hr. The precision of low- and high- surface area measurements was >±0.04 m^2 g^{-1} and <±1.00 m^2 g^{-1}, respectively, based on replicate measurements of surface area Quantachrome instruments standards.

4. Results

4.1. Radiocarbon Content and Ages

Bulk OC-$\Delta^{14}C$ ranges from −130 to −970 ‰ (−462 ‰ on average) and features large spatial variability (Figure 2a and Table S2 in Supporting Information S1). Generally, values decrease from the southwest to the northeast, except for the Gulf of Lions, where several samples show intermediate values. The most ^{14}C-depleted samples (i.e., the oldest OC) are found in the Algero-Provencal Basin (−526 to −970 ‰) and the Gulf of Lions (−503 to −695 ‰). The most ^{14}C-enriched values (i.e., the youngest OC) are found in the Atlantic sector (−235 to −390 ‰) and in the Alboran Sea (−195 to −753 ‰). In the Atlantic sector, the more ^{14}C-depleted values in the Gulf of Cadiz contrast with higher $\Delta^{14}C$ values off the west coast of Portugal. Similarly, samples from the Catalan continental shelf show higher values than those observed in the Valencia Trough.

Conventional (uncalibrated) ^{14}C ages of planktic foraminifera samples range between 500 and 17,470 years BP (Figure 2c and Table S2 in Supporting Information S1). The incorporation of bomb ^{14}C in two samples in the Alboran Sea indicates that foraminifera tests originated after the radiocarbon thermonuclear weapon testing in the 60's. In contrast, four samples in the Balearic Sea and Algero-Provencal Basin show ^{14}C ages >10,000 years.

4.2. Excess ^{210}Pb Concentrations

Samples from the Alboran Sea show highest excess ^{210}Pb concentrations, between 112 and 665 Bq kg^{-1} (Figure 2d). In the Balearic Sea and Gulf of Lions, only the samples from depths <1,800 m have detectable excess ^{210}Pb concentrations (28–115 Bq kg^{-1}), whereas deeper water samples have undetectable excess ^{210}Pb. Similarly, the two analyzed samples from the Algerian Basin do not have any detectable excess ^{210}Pb.

4.3. OM Content and Properties

The $OC_\%$ values ranged from 0.1% to 1.9% (Figure 3a and Table S2 in Supporting Information S1). The highest values are found in the Atlantic sector and Alboran Sea (0.83% and 0.79% on average, respectively) decreasing throughout the Algerian Basin (0.78%), the Balearic Sea (0.71%), and the Algero-Provencal Basin (0.40%). Values in the Gulf of Lions increase up to 0.64% on average.

The $\delta^{13}C$ values range from −21.8 to −27.1 ‰ and show a general decreasing trend toward the northeast, except for the higher values observed in the Gulf of Lions (−22.7 ‰ on average) (Figure 3b and Table S2 in Supporting Information S1). Accordingly, minimum values are found in the Algero-Provencal Basin (−23.8 to −27.2 ‰) while the highest values are found in the Atlantic sector (−22.7 to −23.6 ‰).
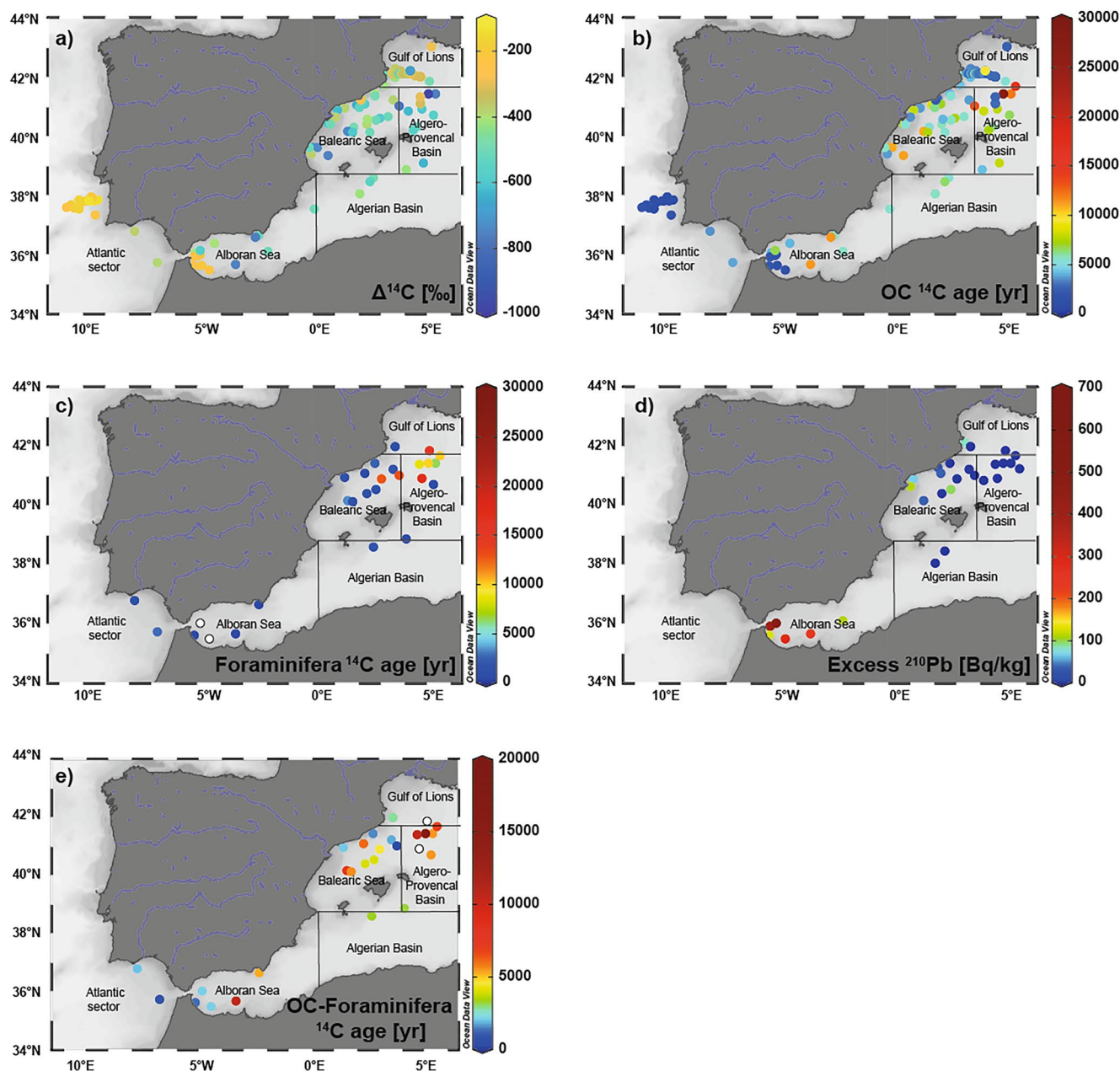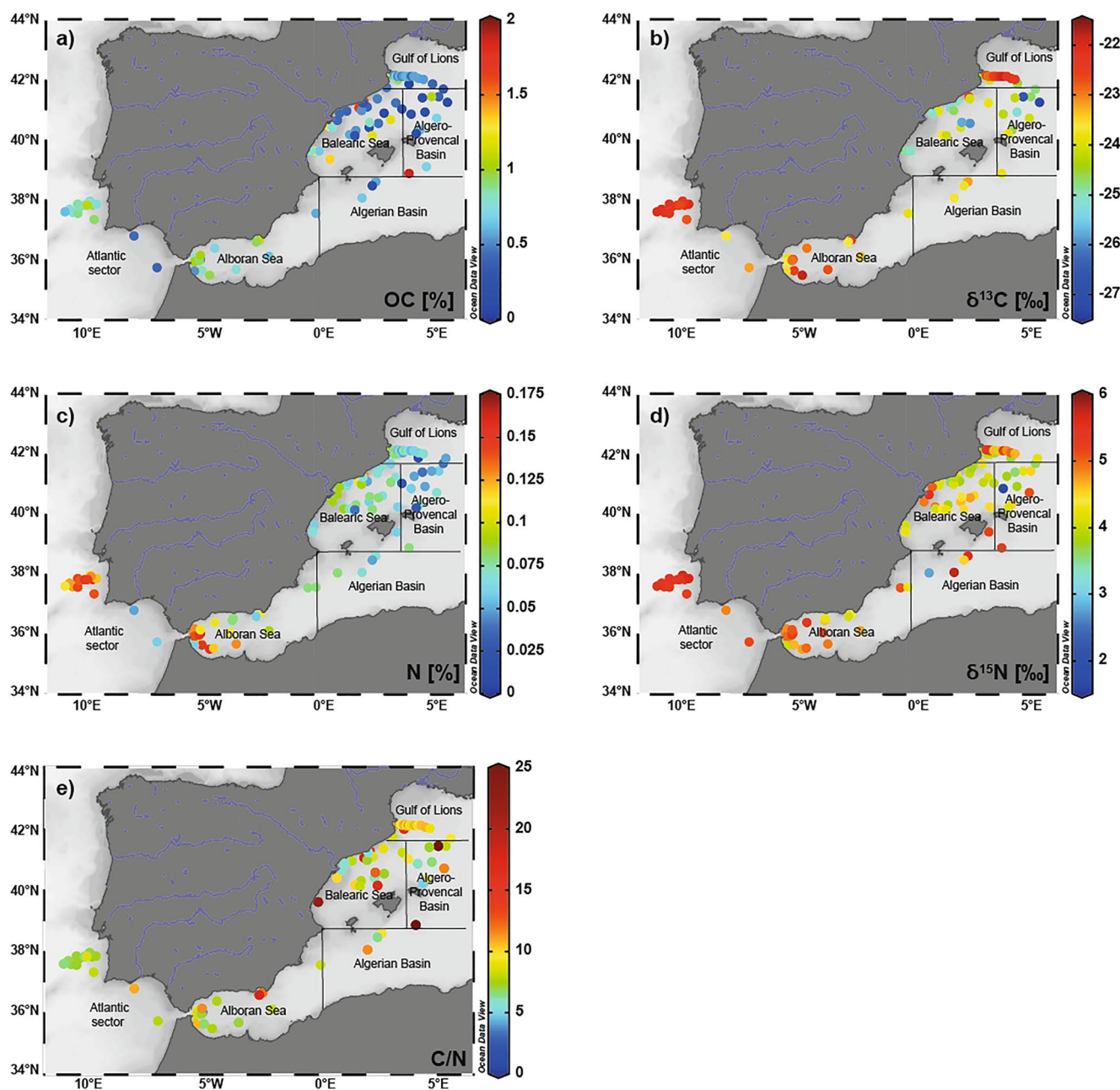
Figure 2. The spatial distribution of sample ages. (a) Radiocarbon content of OC, (b) radiocarbon age of OC, (c) radiocarbon age of planktic foraminifera, (d) excess ^{210}Pb in sediments, and (e) age difference between OC and planktic foraminifera. Note the non-linear color scale in (b–e) to avoid masking of lower values. White circles in panels (c) and (e) represent the incorporation of bomb ^{14}C and negative age differences, respectively. Note that some sample locations overlap (Table S3 in Supporting information S1).

$N_{\%}$ values range between 0.02% and 0.17% and show a gradual southwest to northeast decrease (Figure 3c and Table S2 in Supporting Information S1) with minimum values in the Algero-Provencal Basin and Gulf of Lions (0.05% and 0.07% on average, respectively). The prodelta areas of the Ebro and Llobregat rivers in the Balearic Sea show slightly higher N values than the surrounding samples.

The δ^{15}N values range from 1.8 to 5.8 ‰ and, except for the Gulf of Lions, show an apparent SW-NE decreasing trend (Figure 3d and Table S2 in Supporting Information S1). Surface sediments from the Ebro shelf are enriched by 1 ‰ with respect to nearby sediments.

C/N ratios range from 3.2 to 25 and show a spatially variable distribution within the different basins (Figure 3e and Table S2 in Supporting Information S1). In general, the lowest values are found in the Atlantic sector

Figure 3. The spatial distribution of isotopic and elemental composition of OM. (a) OC content (wt%), (b) stable carbon isotopic composition, (c) total nitrogen content, (d) stable nitrogen isotopic composition, and (e) atomic C/N ratio, with non-linear color scale to avoid masking of lower values. Data from 13 samples in the Gulf of Lions in panels (a–d) are reported elsewhere (Durrieu de Madron et al., 2020).

(6.7–9.3), the Algerian Basin (3.1–15.6), and the Alboran Sea (5.5–9.8), excluding two outliers with a C/N ratio of 25. In contrast, the Balearic Sea and the Algero-Provencal basin show more variable and higher values (5.0–27.2). Samples within the Ebro shelf reveal lower C/N values (~5) than surrounding sediments on the adjacent shelf. The Gulf of Lions shows lower variability (8.9–14.7) and the highest average value (10.5).

4.4. Sedimentological Properties

The median grain-size values range between 5 and 384 μm (Figure 4a and Table S3 in Supporting Information S1). Most samples are mainly composed of silt, with coarse (10–63 μm) and fine silt (2–10 μm) being the greatest contributors (35% and 39% on average, respectively) (Figures 4b–4e and Table S3 in Supporting

Information S1). Grain-size composition is rather homogeneous in the southern region (Atlantic sector, Alboran Sea, and Algerian Basin) with relatively high percentages of total silt (56%–88%). The total silt contribution increases toward the northeast along with a slight increase in the median grain size.

Mineral SA ranges from 1.6 to 44.7 m^2 g^{-1} with a mean of 18 m^2 g^{-1} and shows an apparent decrease toward the northern basins (Figure 4f and Table S3 in Supporting Information S1).

5. Discussion

5.1. Sedimentation Rates and Possible Artifacts During Core Recovery

Low sedimentation rates typically imply lower OC-Δ^{14}C as sediment mixing entrains older carbon from deeper sediment layers. The observed decreasing trend in OC-Δ^{14}C values corresponds to major changes in sedimentation rates across the study area. For instance, sediment accumulation rate is highest in the Alboran Sea (~0.1 cm/yr; Masqué et al., 2003) and decreases toward the Balearic Sea (~0.05 cm/yr; Zuo et al., 1997) and the Gulf of Lions as a function of water depth (0.01–0.65 cm/yr; Miralles et al., 2005). The lowest values are observed in the Algerian basin (0.008 cm/yr; Jimenez-Espejo et al., 2007).

In this regard, the possible partial loss of surface sediments during core recovery would have a larger impact on the measured core-top ages in the north-eastern basins. Many of the oldest samples were retrieved by kasten coring (Figure 1), which, if used correctly, and unlike gravity coring, typically leads to high recoveries of the top few centimeters of the sediment column (Gersonde & Seidenkrantz, 2013). In contrast, box coring and multicoring are assumed to faithfully recover the sediment-water interface. Excess ^{210}Pb is typically used as an indicator of recent sedimentation (<100 years). However, the time elapsed between core retrieval and ^{210}Pb measurements (40-30 years in most cases) limits the detection of excess ^{210}Pb to sites where high concentrations occur naturally (i.e., Atlantic sector, Alboran Sea, and possibly some locations of the Balearic Sea, in agreement with observations (Figure 2d)).

Samples from the Gulf of Lions retrieved by multicorer between 2008 and 2011 (Table S1 in Supporting Information S1) represent only the top half-cm of a multicore (0–0.5 cm) and yet, age range between 2,370 and 9,470 ^{14}C yr (3660 ^{14}C yr, on average) indicating the presence of strongly aged OC even in freshly deposited sediment layers in this region. This finding supports the consistency of the ^{14}C age decrease toward the north-eastern basins regardless of the employed coring device. Moreover, our results are consistent with evidence from three sediment traps deployed in this region that recorded highly depleted OC-Δ^{14}C values (from −653 to −774 ‰) and old ages (~8,500 to ~12,000 years) in the water column (Tesi et al., 2010). These results were attributed to the resuspension and subsequent transport of sediments buried in the upper slope containing fossil OC.

Potential sediment loss during coring also does not explain the large age discrepancies observed between co-deposited foraminifera and OC for these samples, which range from hundreds to several thousands of years (Figure 2e, Table S2 in Supporting Information S1). Older-than-foraminifera OC ages are typically interpreted as resulting from the transport of pre-aged/fossil OC to the study site (e.g., Mollenhauer et al., 2005; Ohkouchi et al., 2002). OC is older than foraminifera in most of the samples, and the magnitude of this discrepancy increases toward the NE, supporting the idea that the input of pre-aged/fossil OC is higher in this region. Two samples in the NE show younger-than-foraminifera OC ages (Figure 2e), a phenomenon typically ascribed to post-depositional processes such as bioturbation (Ausín et al., 2019). Values of surface mixed layer depth are spatially distinct in the NE, ranging from high (up to 30 cm) near the Rhone and down to <0.5 cm offshore (Zuo et al., 1997), where these two samples are located. However, additional factors such as decreased foraminifera production, shell fragmentation, or lateral displacement of foraminifera tests by strong currents may have contributed to the magnitude of the observed negative age differences in these two samples (ca. 10,000 ^{14}C yr).

Overall, while potential sediment loss in some samples cannot be discounted, such potential artifacts cannot explain the geochemical gradients that emerge from these data (Figure 5), which are indeed coherent with the main biological, hydrological, and sedimentological changes that occur along the ^{14}C age gradient (Section 5.3). Thus, an interplay of factors including lower vertical flux of fresh OM, lower sedimentation rates, and higher input of fossil and pre-aged OC by rivers and re-exposed sediments may have determined the observed geochemical and sedimentological spatial patterns.
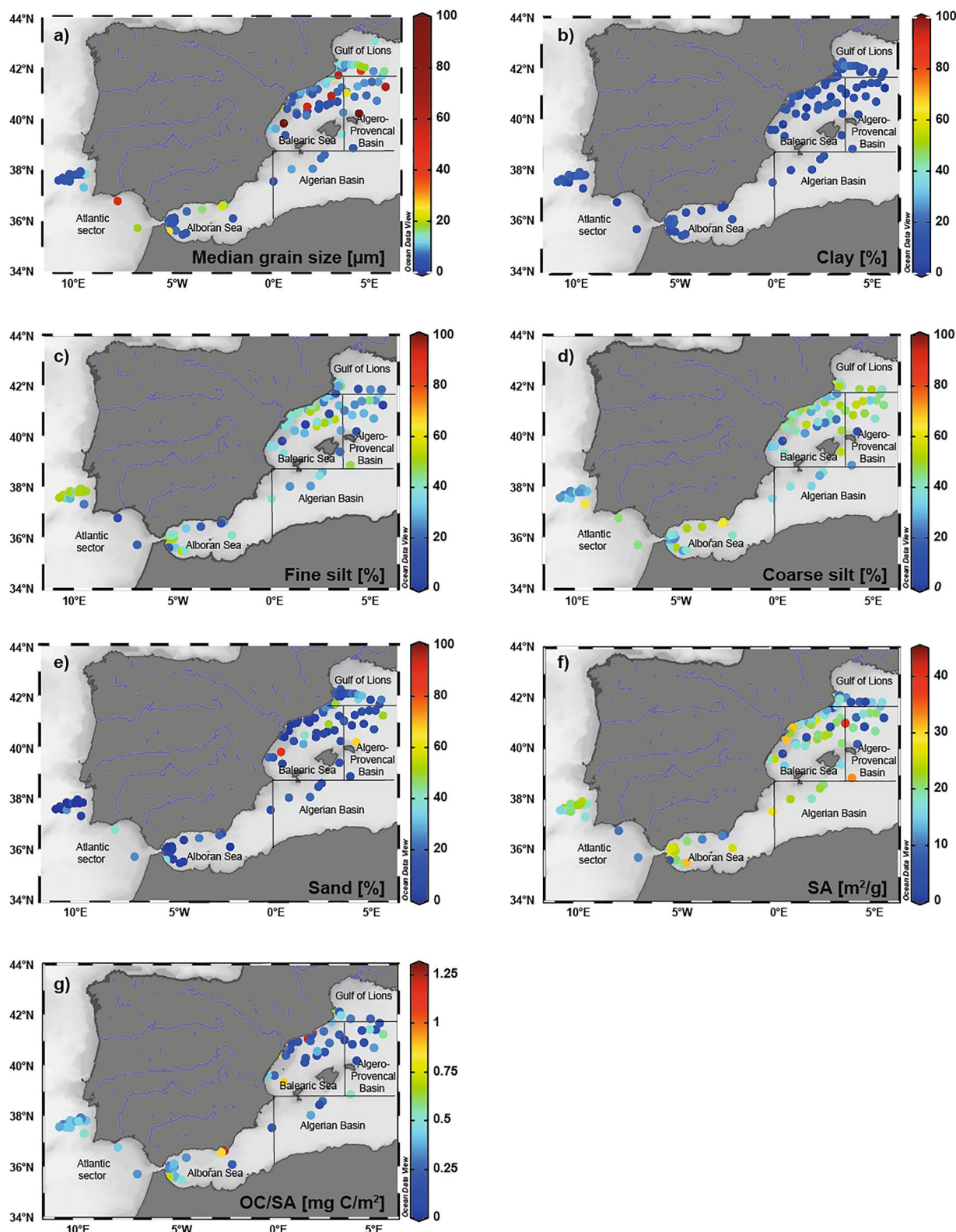
Figure 4. Grain-size composition. (a) Median grain size with non-linear color scale to avoid masking of lower values. Relative abundance of (b) clay, (c) fine silt, (d) coarse silt, and (e) sand. (f) Mineral surface area and (g) OC loadings normalized to mineral surface area.
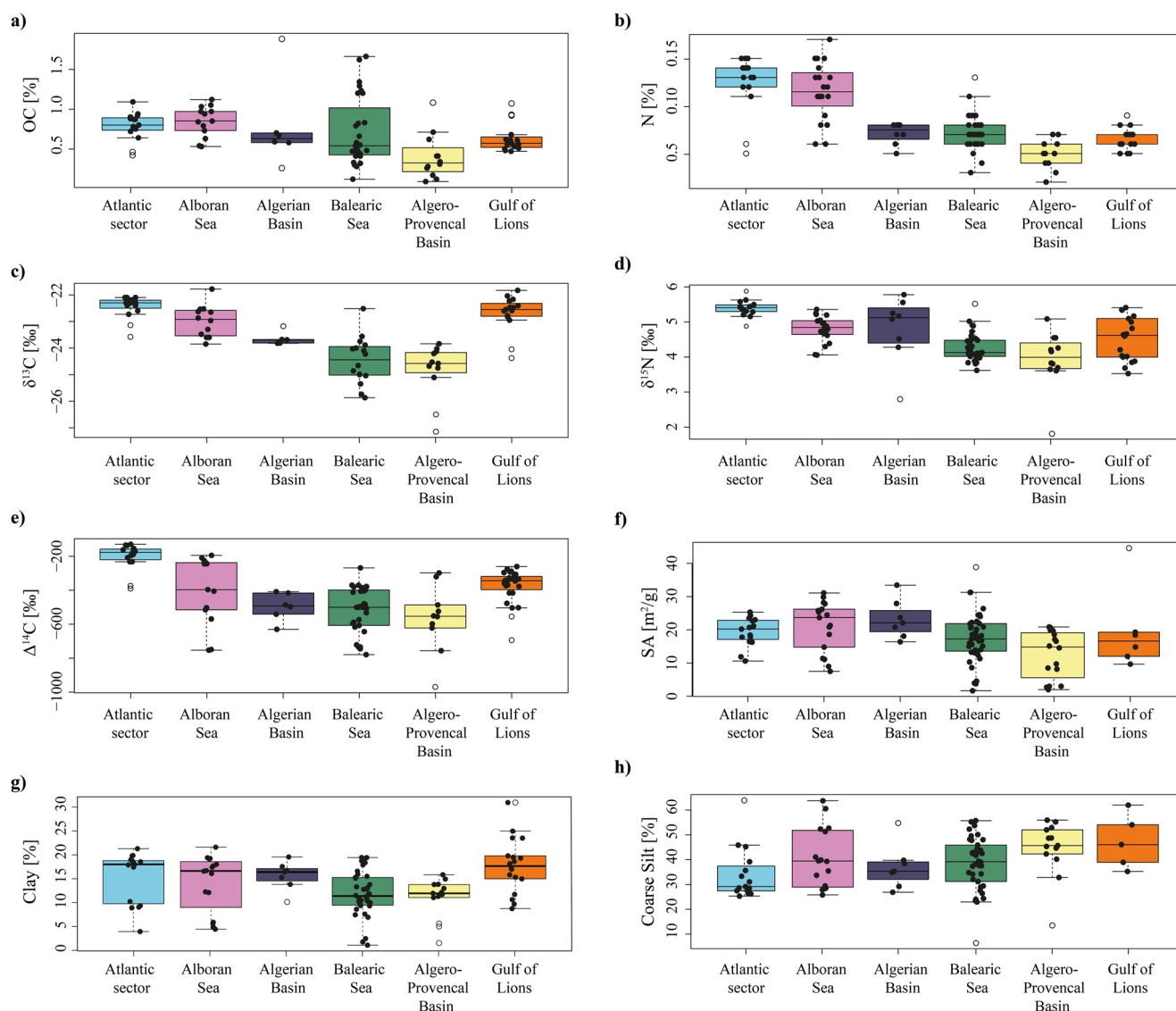
Figure 5. The boxplot of the main geochemical and sedimentological characteristics of OM within each basin, shown from the SW to the NE of the study area. (a) OC content (wt%), (b) nitrogen content, (c) stable carbon isotopes of OC, (d) stable nitrogen isotopes, (e) radiocarbon content of OC, (f) mineral surface area, (g) clay and (h) coarse silt relative abundance. Black dots represent the values for each sample. The solid black line is the median and the upper and lower limits of the box represent the interquartile range (25%–75%). Open circles indicate potential outliers.

5.2. Geochemical and Sedimentological Spatial Patterns

An apparent SW-NE gradient is observed in most of the geochemical and sedimentological features (Figures 5a–5h), which generally show a decreasing trend toward the north-eastern basins. However, an exception to these trends is found in samples collected from the Gulf of Lions. In this region, a notable trend reversal is observed in most parameters, as illustrated in Figures 5a–5e and 5g.

Specifically, samples from the south-western basins (i.e., the Atlantic sector and Alboran Sea) exhibit higher median $OC_\%$ and $N_\%$, higher median $\delta^{13}C$, $\delta^{15}N$, and $\Delta^{14}C$ values, and higher median mineral SA and relative abundance of clay than those from the Balearic Sea and the Algero-Provencal Basin.

5.3. Major Biological and Hydrological Controls on the Spatial Distribution of the Geochemical Characteristics of OM

The spatial variability observed in the elemental and stable isotopic composition of OM indicates regional differences in the relative proportions of marine and terrestrial OM (Rau et al., 1989; Wada & Hattori, 1991). These,
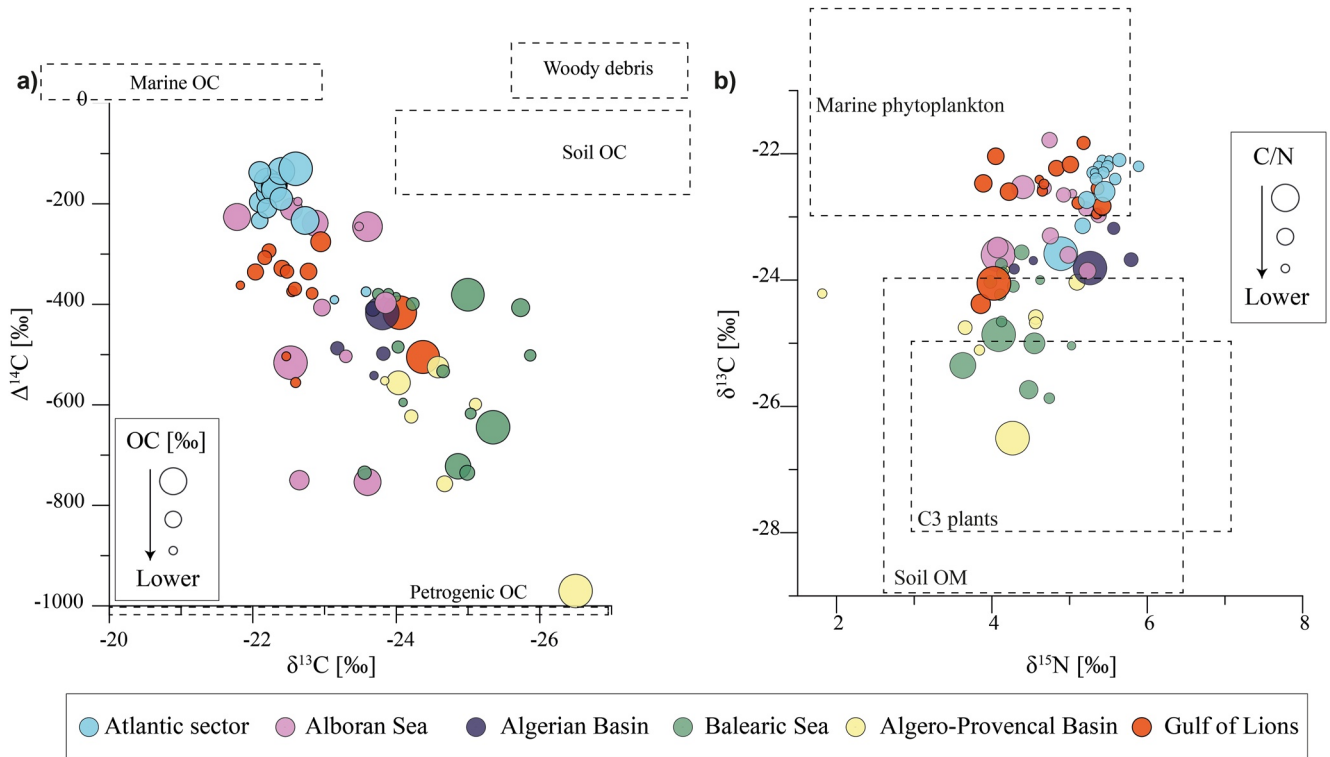
Figure 6. Isotopic composition of OM. (a) Radiocarbon content versus $\delta^{13}C$ with OC content as normalized bubble size, and (b) $\delta^{13}C$ versus $\delta^{15}N$ with atomic C/N ratios as normalized bubble size. Dashed boxes indicate the main endmembers: marine phytoplankton (Verwega et al., 2021), soil OM (McCallister et al., 2004; Ogrinc et al., 2008), and dominant Mediterranean vegetation (C3 plants; Countway et al., 2007; Hedges et al., 1997; Ogrinc et al., 2008).

in turn, reflect the major biological and hydrological processes that characterize the study area. For instance, the spatial gradient in $OC_\%$ (Figure 5a) parallels that of primary productivity as evidenced by ocean color satellite data (Bosc et al., 2004; D'Ortenzio & Ribera d'Alcalà, 2009) and model analysis (Colella et al., 2016; Lazzari et al., 2012).

In the south-western basins (Atlantic sector and Alboran Sea), higher $OC_\%$ can be largely explained by enhanced vertical settling of local and freshly produced OM. In agreement, sedimentary OC from these basins is of primarily marine origin and relatively young (higher OC-$\Delta^{14}C$ values) (Figure 6a). Here, higher $\delta^{13}C$ and lower C/N values agree with typical values of marine phytoplankton for northern mid-latitudes (−20 and −22.5 ‰ (Verwega et al., 2021) and ∼7 (Liang et al., 2019; Meyers, 1994), respectively). The Atlantic sector is part of a major upwelling region, whereas the primary production in the Alboran Sea is one of the highest in the Mediterranean Sea (Lazzari et al., 2012). Moreover, the major rivers in this region have smaller drainage basins and lower discharge volumes in relation to the major northern rivers (Ebro and Rhone), and except for the Almeria canyon, canyons are not as well developed in this southern region (Würtz, 2012). Altogether, these factors diminish the potential input of terrestrial OC.

By contrast, the OC content gradually decreases and ages toward the NE (Figure 6a). This pattern is explained by reduced primary productivity and increased input of terrestrial OM throughout the Algerian Basin, the Balearic Sea, and the Algero-Provencal Basin. Resuspension and lateral transport of fine sediments by strong deep currents can expose mineral-associated OC to further alteration, leading to the preferential degradation of more labile (younger and predominantly marine) OC in relation to the more refractory (older material including terrestrial) OC (Bao et al., 2016; Tesi et al., 2007). However, the observed extremely low $\Delta^{14}C$ values (−381 to −970 ‰) cannot solely be explained by aging during resuspension and lateral transport. These values instead likely indicate the input of fossil/petrogenic (^{14}C-depleted) OC, mainly of terrestrial origin (Figure 6b). Indeed, numerous rivers discharging into this region are responsible for the entrainment of large amounts of terrestrial OM in the north-eastern basins. The biochemical characterization over a 1 year period of the particulate OM delivered by 8 major and minor rivers discharging into the Gulf of Lions and the Catalan shelf showed $\delta^{13}C$ values ranging from

−33 to −24.5 ‰, δ^{15}N values between 1.9 and 16.8 ‰, and C/N values from 2.8 to 14.7 (Higueras et al., 2014). According to Higueras et al. (2014), such values reflect the admixture of soil OM (McCallister et al., 2004; Ogrinc et al., 2008) and vascular C3 plant remains (Countway et al., 2007; Hedges et al., 1997; Ogrinc et al., 2008).

Weathering and supply of terrestrial OC to the Balearic Sea by the Rhone and Ebro rivers is typically limited to the shelf (Arnau et al., 2015; Palanques et al., 2006). However, the presence of large submarine canyons on the Catalan shelf compared to the margins of the south-western basins and the seaward deflection of the coastal current at the southern limit of the Valencia Trough (Figure 1) deliver large quantities of sedimentary OM to deeper waters (Arnau et al., 2015; Ulses et al., 2008). Similarly, fish trawling activity, which influences the sedimentary OM distribution through sediment erosion and enhanced OC remineralization (Palanques et al., 2014; Paradis, Lo Iacono, et al., 2021), is limited to the shelf and upper slope of the Catalan margin. Nevertheless, onshore and offshore δ^{13}C values are comparable (Figure 3b), suggesting the input of terrestrial OC through mass movement events and strong along-slope and upslope currents around the Balearic Island (Lüdmann et al., 2012) and the efficient transport of sedimentary OM along the basin in the Valencia Trough (Amblas et al., 2011; O'Connell et al., 1985). Slightly enhanced N$_\%$ and δ^{15}N values in the proximity of the mouth of the Ebro River have been ascribed to the delivery of synthetic fertilizer products derived from agricultural activities (Lassaletta et al., 2012), enabled by the dense irrigation channels and reservoirs in the catchment area of the Ebro (<400 kg N km^{-2} yr^{-1}) (Romero et al., 2016).

In the Gulf of Lions, relatively higher Δ^{14}C and δ^{13}C (Figure 6a) values reflect higher contribution of marine OM linked to increased primary productivity compared to other north-eastern basins of the NW Mediterranean Sea (Bosc et al., 2004; Colella et al., 2016; D'Ortenzio & Ribera d'Alcalà, 2009). Δ^{14}C and stable isotopic values of OM agree with previous observations and suggest the admixture of OC from different sources (Sanchez-Vidal et al., 2009; Tesi et al., 2010). In addition to the intense seasonal planktonic bloom that characterizes this region, fluvial discharges by major and minor rivers imply the entrainment of large amounts of terrestrial OC (Higueras et al., 2014). Previous work has shown the alternation between sedimentary OC sources in the Gulf of Lions, being predominantly terrestrial during winter, and mainly marine during spring and summer (Sanchez-Vidal et al., 2009). Re-exposure and advection of sediments deposited during low sea-level stands and buried on the upper continental slope are an additional source of pre-aged/fossil OC in this region (Tesi et al., 2010). Finally, resuspension and dispersal of sediments by deep currents following bottom-reaching convection events in this region (Durrieu de Madron et al., 2017; Stabholz et al., 2013) further contributes to the mixing of freshly produced marine OM and older terrestrial OM (Canals et al., 2006; Sanchez-Vidal et al., 2009).
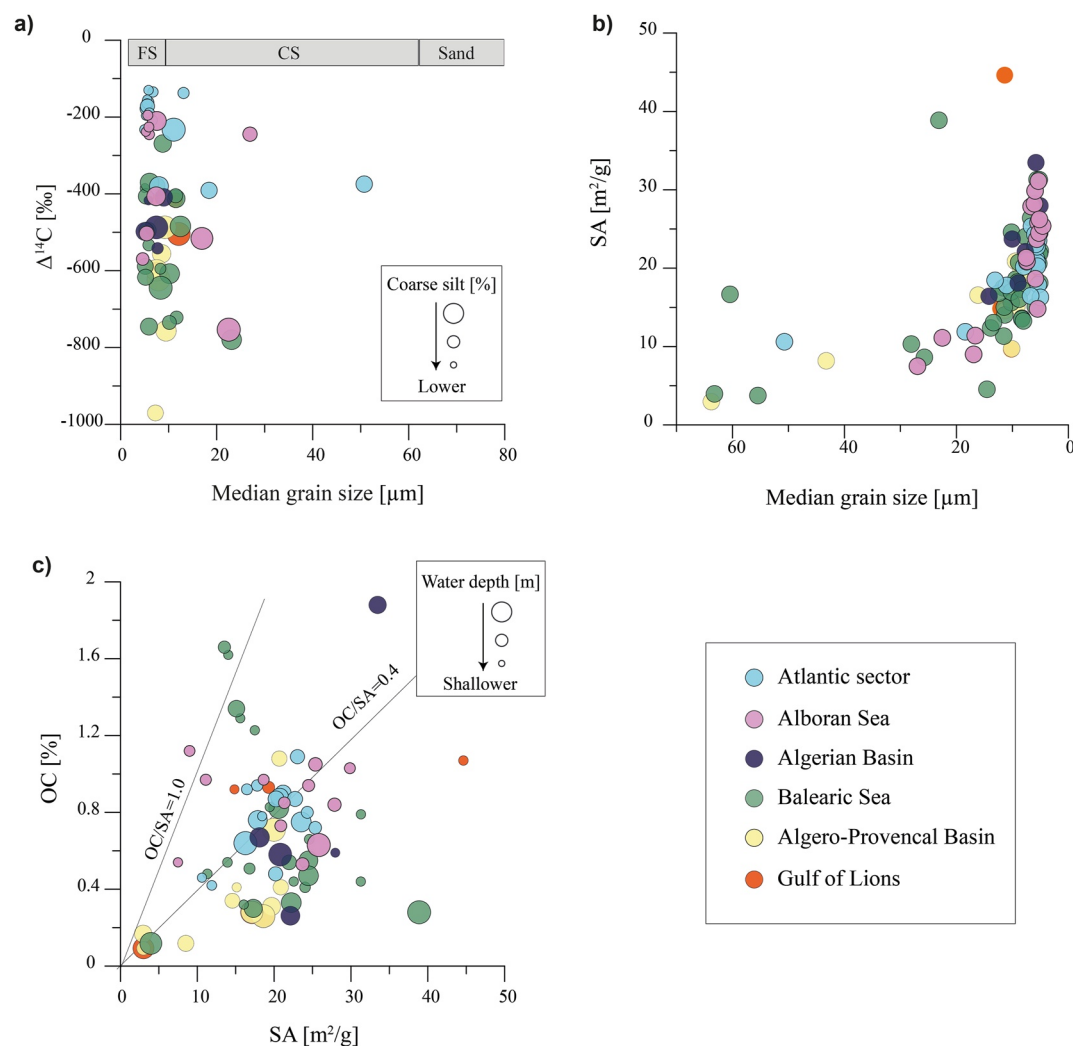
5.4. Potential Additional Controls on the Distribution and Fate of OM Via Organo-Mineral Associations

5.4.1. Lateral Transport of Allochthonous OC

Substantial and positive age differences between co-deposited OC and planktic foraminifera increase toward the NE and are mainly ascribed to the addition of old OC (Section 5.1). Although the origin of this OC appears to be predominantly terrestrial, the contribution of laterally transported pre-aged/fossil OC of marine origin in association with mineral grains has been observed in the region (Tesi et al., 2010) and could have contributed to the observed age differences to some extent.

Moreover, OM may age during resuspension/redeposition cycles (Bao et al., 2016) because selective degradation of the more labile organic molecules over the more refractory material occurs under oxic conditions and lateral transport leads to an increase in oxygen exposure times (Burdige, 2007; Hedges et al., 1999). Recently produced marine OM is more prone to remineralization potentially as a consequence of its chemically labile and less altered nature compared to terrestrial OM (Zonneveld et al., 2010). Similarly, previous work in the Gulf of Lions has shown that sedimentary OM along a mud belt on the shelf is much more depleted in ^{14}C than in the delta region due to the preferential loss of labile OM and retention of fossil carbon during resuspension and lateral transport (Cathalot et al., 2013; Tesi et al., 2007). Thus, preferential degradation of freshly produced marine OC could also have contributed to the observed terrestrial signal toward the NE basins.

Finally, hydrodynamic mineral sorting during lateral transport leads to a strong ^{14}C age-grain-size dependence (Ausín et al., 2021). The spatial changes observed in the relative contribution of clay and sortable silt (Figures 5g and 5h) suggest that hydrodynamically-sorted minerals that host OC could contribute to some extent to the observed Δ^{14}C, which decreases toward the NE (except in the Gulf of Lions) along with a decrease in clay relative

Figure 7. Additional controls on the distribution and fate of OM. (a) Relationship between $\Delta^{14}C$ and median grain size with coarse silt (10–63 μm) relative abundance as normalized bubble size, (b) relationship between mineral surface area and median grain size, and (c) OC content versus mineral surface area with water depth as normalized bubble size. FS = Fine silt. CS = Coarse silt. Solid lines in (b) indicate OC/SA ratios >1 and <0.4 mg OC m^{-2}, which allow the differentiation of depositional environments (Bianchi et al., 2018; Blair & Aller, 2012).

abundance and an increase in coarse silt percentage. However, as in other marginal seas, no apparent relationship is observed between $\Delta^{14}C$ and median grain size in samples dominated by fine-grained sediments (<63 μm, Figure 7a) because the $\Delta^{14}C$-grain-size relationship is only apparent when investigated across grain-size fractions (Bao et al., 2016).

5.4.2. OM Protection Via Association With Mineral Surfaces

Minerals influence the abundance and geochemical composition of sedimentary OC via mineral SA protection (Keil et al., 1994). Finer mineral grains offer higher SA (Figure 7b); spaces where the OM may be occluded and OC is protected from remineralization by heterotrophic organisms (Bianchi et al., 2018). Accordingly, OC preservation would be comparatively lower in the Balearic Sea and Algero-Provencal Basin (Figures 5f and 7b) because lower SA would expose OM to selective degradation (Zonneveld et al., 2010).

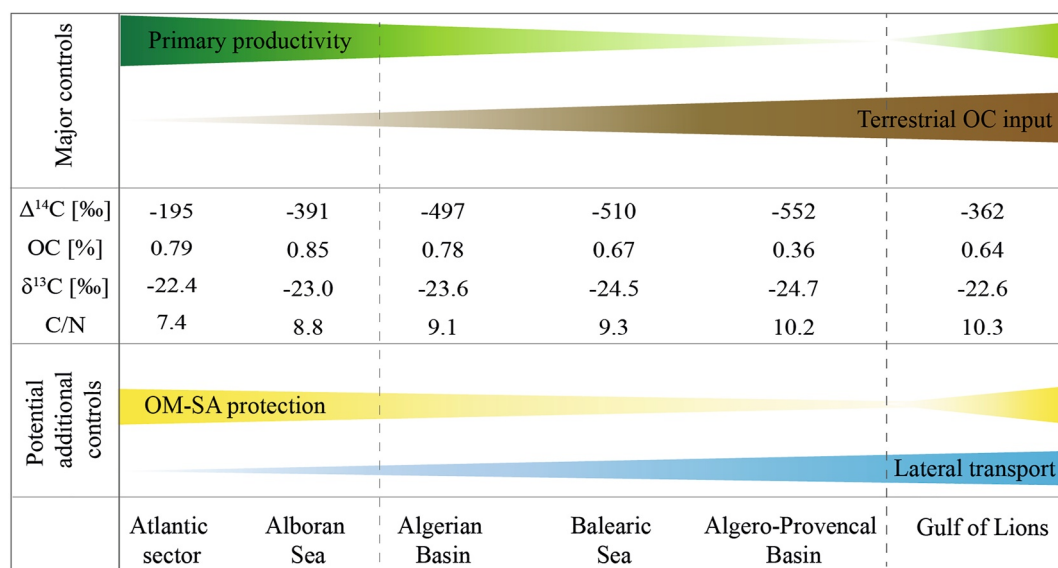SA does not follow the SW-NE gradient observed in other geochemical and sedimentological parameters because it is not the highest on the Atlantic side. The latter suggest a lower potential for OM protection by mineral surfaces in the Atlantic sector. However, the OC/SA ratio allows the assessment of net supply and reaction processes of OC and preservation efficiency (Blair & Aller, 2012). Most OC/SA values are <0.4 mg C m^{-2}

(Figure 7c). This is especially the case for the majority of the samples from the Algerian Sea, Balearic Sea, and Algero-Provencal Basin, with few exceptions to shallower waters from the Balearic Sea that show an OC/SA ratio between 1 and 0.4 mg C m^{-2}. OC/SA values <0.4 mg C m^{-2} are characteristic of passive continental margins and environments where sediment is frequently resuspended and subjected to enhanced remineralization (e.g., highly energetic deltaic deposits and low-sedimentation-rate deep-sea environments with long oxygen exposure times) (Bao et al., 2018; Blair & Aller, 2012). Samples from the Atlantic Sector and the Alboran Sea, on the other hand, show comparatively higher OC/SA values, and more than half of them show ratios in the 1–0.4 mg C m^{-2} range. These values are characteristic of river-suspended material and shelf sediments and indicate relatively stable OM-mineral associations that prevent OC from further remineralization (Blair & Aller, 2012; Hedges & Keil, 1995). Therefore, our results suggest that the potential for OM protection by mineral surfaces is larger in the Atlantic sector and Alboran Sea, and lower in the Balearic Sea and Algero-Provencal Basin. In the absence of other factors that have also proven to play an important role in OM protection-like sediment mineralogy (Blattmann et al., 2019), mineral surface area protection would magnify the observed geochemical gradients.

6. Conclusions

This regional study on the isotopic and elemental composition of OM in surface sediments from the western Mediterranean Sea and the neighboring Atlantic sector west of the Strait of Gibraltar sheds light on the controls on the origin, distribution, and fate of OM in continental margins and adjacent deep-sea basins.

Here, most geochemical parameters depict a clear SW-NE gradient that reverses in the Gulf of Lions (Figure 8). Thus, samples from the Atlantic sector and Alboran Sea reveal comparatively younger OM that is primarily of marine origin. Samples from the Algerian Basin, the Balearic Sea, and the Algero-Provencal Basin exhibit a larger influence of terrestrial OC toward the NE characterized by lower δ^{13}C and ^{14}C values. OM in the Gulf of Lions shows a more prominent influence of fresh and young OC compared to other basins in the north-eastern part of the NW Mediterranean Sea. Such spatial variability largely reflects regional differences in relation to marine primary productivity and terrestrial input of pre-aged/fossil OC, the latter delivered by rivers and channeled to the deeper basin by the numerous canyons that incise the continental margin, especially toward the NE of the study area.

	Atlantic sector	Alboran Sea	Algerian Basin	Balearic Sea	Algero-Provencal Basin	Gulf of Lions
Δ^{14}C [‰]	-195	-391	-497	-510	-552	-362
OC [%]	0.79	0.85	0.78	0.67	0.36	0.64
δ^{13}C [‰]	-22.4	-23.0	-23.6	-24.5	-24.7	-22.6
C/N	7.4	8.8	9.1	9.3	10.2	10.3

Figure 8. A conceptual model summarizing the influence of major and potential additional controls on the geochemical characteristics of sedimentary OM in the Western Mediterranean Sea and adjacent Atlantic sector, from the SW to the NE. Values of the main geochemical parameters correspond to the bound mean values (10%) of each basin. Note the SW-NE gradient, which reverses in the Gulf of Lions.

When explored a sedimentological context, our results reveal the potential secondary control of two other mechanisms on the fate of OM (Figure 8). The first involves the resuspension and lateral transport of allochthonous (mainly pre-aged or fossil) OC in association with fine-grained sediments. The increasing contribution of coarse silt toward the NE basins suggests that the impact of this mechanism is potentially greatest in the north-eastern basins, where intense high-energy events promote grain-size sorting and its subsequent sediment (and OC) redistribution. Moreover, lateral transport would further expose OM to oxic conditions, favoring selective degradation of labile OC over refractory OC. The other potential secondary control in the fate of OM is OM protection from oxic degradation via association with mineral surfaces. This mechanism would have a larger influence in the Atlantic sector and Alboran Sea due to comparatively higher OC/SA ratios in these basins. In the Balearic Sea and Algero-Provencal Basin, lower OM protection by mineral surfaces would potentially lead to lower $OC_\%$ and the preferential retention of more refractory terrestrial OC that renders bulk OC strongly depleted in ^{14}C, in line with the observed geochemical gradients.

Overall, the spatial heterogeneity exhibited by the western Mediterranean Sea allows us to explore the interplay of biological, chemical, and hydrological factors that control the amount and geochemical characteristics of sedimentary OM in continental margins, including the land-sea continuum and the deeper ocean.

Data Availability Statement

All the underlying data needed to understand, evaluate, and build on the reported research is in Supporting Information S1 and accessible online in the Mendeley public repository under Ausín et al. (2023) https://doi.org/10.17632/5rvgcz5ynh.1.

References

Amblas, D., Gerber, T. P., Canals, M., Pratson, L. F., Urgeles, R., Lastras, G., & Calafat, A. M. (2011). Transient erosion in the Valencia Trough turbidite systems, NW Mediterranean basin. *Geomorphology*, *130*(3–4), 173–184. https://doi.org/10.1016/j.geomorph.2011.03.013

Arjona-Camas, M., Puig, P., Palanques, A., Durán, R., White, M., Paradis, S., & Emelianov, M. (2021). Natural vs. trawling-induced water turbidity and suspended sediment transport variability within the Palamós Canyon (NW Mediterranean). *Marine Geophysical Researches*, *42*(4), 38. https://doi.org/10.1007/s11001-021-09457-7

Arnau, P., Liquete, C., & Canals, M. (2015). River mouth plume events and their dispersal in the northwestern Mediterranean Sea. *Oceanography*, *17*(3), 22–31. https://doi.org/10.5670/oceanog.2004.27

Atwood, T. B., Witt, A., Mayorga, J., Hammill, E., & Sala, E. (2020). Global patterns in marine sediment carbon stocks. *Frontiers in Marine Science*, *7*. https://doi.org/10.3389/fmars.2020.00165

Ausín, B., Bossert, G., Krake, N., Paradis, S. H. N., Durrieu de Madron, X., Alonso, B., & Eglinton, T. (2023). Geochemical and sedimentological signals from surface sediment samples from the Western Mediterranean Sea and adjacent Atlantic sector. *Mendeley Data. V1*. https://doi.org/10.17632/5rvgcz5ynh.1

Ausín, B., Bruni, E., Haghipour, N., Welte, C., Bernasconi, S. M., & Eglinton, T. I. (2021). Controls on the abundance, provenance and age of organic carbon buried in continental margin sediments. *Earth and Planetary Science Letters*, *558*, 116759. https://doi.org/10.1016/j.epsl.2021.116759

Ausín, B., Haghipour, N., Wacker, L., Voelker, A. H. L., Hodell, D., Magill, C., et al. (2019). Radiocarbon age offsets between two surface dwelling planktonic foraminifera species during abrupt climate events in the SW Iberian Margin. *Paleoceanography and Paleoclimatology*, *34*(1), 63–78. https://doi.org/10.1029/2018pa003490

Bao, R., McIntyre, C., Zhao, M., Zhu, C., Kao, S.-J., & Eglinton, T. I. (2016). Widespread dispersal and aging of organic carbon in shallow marginal seas.

Bao, R., van der Voort, T. S., Zhao, M., Guo, X., Montluçon, D. B., McIntyre, C., & Eglinton, T. I. (2018). Influence of hydrodynamic processes on the fate of sedimentary organic matter on continental margins. *Global Biogeochemical Cycles*, *32*(9), 1420–1432. https://doi.org/10.1029/2018gb005921

Bianchi, T. S., Cui, X., Blair, N. E., Burdige, D. J., Eglinton, T. I., & Galy, V. (2018). Centers of organic carbon burial and oxidation at the land-ocean interface. *Organic Geochemistry*, *115*, 138–155. https://doi.org/10.1016/j.orggeochem.2017.09.008

Blair, N. E., & Aller, R. C. (2012). The fate of terrestrial organic carbon in the marine environment. *Annual Review of Marine Science*, *4*(1), 401–423. https://doi.org/10.1146/annurev-marine-120709-142717

Blattmann, T. M., Liu, Z., Zhang, Y., Zhao, Y., Haghipour, N., Montluçon, D. B., et al. (2019). Mineralogical control on the fate of continentally derived organic matter in the ocean. *Science*, *366*(6466), 742–745. https://doi.org/10.1126/science.aax5345

Bosc, E., Bricaud, A., & Antoine, D. (2004). Seasonal and interannual variability in algal biomass and primary production in the Mediterranean Sea, as derived from 4 years of SeaWiFS observations. *Global Biogeochemical Cycles*, *18*(1), GB1005. https://doi.org/10.1029/2003gb002034

Bricaud, A., Bosc, E., & Antoine, D. (2002). Algal biomass and sea surface temperature in the Mediterranean Basin: Intercomparison of data from various satellite sensors, and implications for primary production estimates. *Remote Sensing of Environment*, *81*(2–3), 163–178. https://doi.org/10.1016/s0034-4257(01)00335-2

Bröder, L., Tesi, T., Andersson, A., Semiletov, I., & Gustafsson, Ö. (2018). Bounding cross-shelf transport time and degradation in Siberian-Arctic land-ocean carbon transfer. *Nature Communications*, *9*(1), 806. https://doi.org/10.1038/s41467-018-03192-1

Bruni, E. T., Blattmann, T. M., Haghipour, N., Louw, D., Lever, M., & Eglinton, T. I. (2022). Sedimentary hydrodynamic processes under low-oxygen conditions: Implications for past, present, and future oceans. *Frontiers in Earth Science. Hypothesis and Theory*, *10*. https://doi.org/10.3389/feart.2022.886395

Burdige, D. J. (2007). Preservation of organic matter in marine sediments: Controls, Mechanisms, and an imbalance in sediment organic carbon budgets? *Chemical Reviews*, *107*(2), 467–485. https://doi.org/10.1021/cr050347q

Canals, M., Company, J. B., Martín, D., Sànchez-Vidal, A., & Ramírez-Llodrà, E. (2013). Integrated study of Mediterranean deep canyons: Novel results and future challenges. *Progress in Oceanography*, *118*, 1–27. https://doi.org/10.1016/j.pocean.2013.09.004

Canals, M., Puig, P., de Madron, X. D., Heussner, S., Palanques, A., & Fabres, J. (2006). Flushing submarine canyons. *Nature*, *444*(7117), 354–357. https://doi.org/10.1038/nature05271

Cathalot, C., Rabouille, C., Tisnérat-Laborde, N., Toussaint, F., Kerhervé, P., Buscail, R., et al. (2013). The fate of river organic carbon in coastal areas: A study in the Rhône river delta using multiple isotopic (δ^{13}C, Δ^{14}C) and organic tracers. *Geochimica et Cosmochimica Acta*, *118*, 33–55. https://doi.org/10.1016/j.gca.2013.05.001

Colella, S., Falcini, F., Rinaldi, E., Sammartino, M., & Santoleri, R. (2016). Mediterranean ocean colour chlorophyll trends. *PLoS One*, *11*(6), e0155756. https://doi.org/10.1371/journal.pone.0155756

Countway, R. E., Canuel, E. A., & Dickhut, R. M. (2007). Sources of particulate organic matter in surface waters of the York River, VA estuary. *Organic Geochemistry*, *38*(3), 365–379. https://doi.org/10.1016/j.orggeochem.2006.06.004

D'Ortenzio, F., & Ribera d'Alcalà, M. (2009). On the trophic regimes of the Mediterranean Sea: A satellite analysis. *Biogeosciences*, *6*(2), 139–148. https://doi.org/10.5194/bg-6-139-2009

Durrieu de Madron, X., Aubert, D., Charrière, B., Kunesch, S., Menniti, C., Radakovitch, O., & Sola, J. (2023). Impact of dense water formation on the transfer of particles and trace metals from the coast to the deep in the northwestern Mediterranean. *Water*, *15*(2), 301. https://doi.org/10.3390/w15020301

Durrieu de Madron, X., Ramondenc, S., Berline, L., Houpert, L., Bosse, A., Martini, S., et al. (2017). Deep sediment resuspension and thick nepheloid layer generation by open-ocean convection. *Journal of Geophysical Research: Oceans*, *122*(3), 2291–2318. https://doi.org/10.1002/2016jc012062

Durrieu de Madron, X., Stabholz, M., HeimbÜRger-Boavida, L.-E., Aubert, D., KerhervÉ, P., & Ludwig, W. (2020). Approaches to evaluate spatial and temporal variability of deep marine sediment characteristics under the impact of dense water formation events. *Mediterranean Marine Science*, *21*, 527–544. https://doi.org/10.12681/mms.22581

García, M., Alonso, B., Ercilla, G., & Gràcia, E. (2006). The tributary valley systems of the Almeria canyon (Alboran Sea, SW Mediterranean): Sedimentary architecture. *Marine Geology*, *226*(3–4), 207–223. https://doi.org/10.1016/j.margeo.2005.10.002

Gersonde, R., & Seidenkrantz, M.-S. (2013). Sampling marine sediment. PAGES past global changes (Vol. *21*, pp. 8–9).

Hedges, J. I., Hu, F. S., Devol, A. H., Hartnett, H. E., Tsamakis, E., & Keil, R. G. (1999). Sedimentary organic matter preservation; a test for selective degradation under oxic conditions. *American Journal of Science*, *299*(7–9), 529–555. https://doi.org/10.2475/ajs.299.7-9.529

Hedges, J. I., & Keil, R. G. (1995). Sedimentary organic matter preservation: An assessment and speculative synthesis. *Marine Chemistry*, *49*(2–3), 81–115. https://doi.org/10.1016/0304-4203(95)00013-h

Hedges, J. I., Keil, R. G., & Benner, R. (1997). What happens to terrestrial organic matter in the ocean? *Organic Geochemistry*, *27*(5–6), 195–212. https://doi.org/10.1016/s0146-6380(97)00066-1

Hemingway, J. D., Rothman, D. H., Grant, K. E., Rosengard, S. Z., Eglinton, T. I., Derry, L. A., & Galy, V. V. (2019). Mineral protection regulates long-term global preservation of natural organic carbon. *Nature*, *570*(7760), 228–231. https://doi.org/10.1038/s41586-019-1280-6

Higueras, M., Kerhervé, P., Sanchez-Vidal, A., Calafat, A., Ludwig, W., Verdoit-Jarraya, M., et al. (2014). Biogeochemical characterization of the riverine particulate organic matter transferred to the NW Mediterranean Sea. *Biogeosciences*, *11*(1), 157–172. https://doi.org/10.5194/bg-11-157-2014

Jimenez-Espejo, F. J., Martinez-Ruiz, F., Sakamoto, T., Iijima, K., Gallego-Torres, D., & Harada, N. (2007). Paleoenvironmental changes in the western Mediterranean since the last glacial maximum: High resolution multiproxy record from the Algero–Balearic basin. *Palaeogeography, Palaeoclimatology, Palaeoecology*, *246*(2–4), 292–306. https://doi.org/10.1016/j.palaeo.2006.10.005

Keil, R. G., Tsamakis, E., Fuh, C. B., Giddings, J. C., & Hedges, J. I. (1994). Mineralogical and textural controls on the organic composition of coastal marine sediments: Hydrodynamic separation using SPLITT-fractionation. *Geochimica et Cosmochimica Acta*, *58*(2), 879–893. https://doi.org/10.1016/0016-7037(94)90512-6

Kessouri, F., Ulses, C., Estournel, C., Marsaleix, P., D'Ortenzio, F., Severin, T., et al. (2018). Vertical mixing effects on phytoplankton dynamics and organic carbon export in the western Mediterranean Sea. *Journal of Geophysical Research: Oceans*, *123*(3), 1647–1669. https://doi.org/10.1002/2016jc012669

Lassaletta, L., Romero, E., Billen, G., Garnier, J., García-Gómez, H., & Rovira, J. V. (2012). Spatialized N budgets in a large agricultural Mediterranean watershed: High loading and low transfer. *Biogeosciences*, *9*(1), 57–70. https://doi.org/10.5194/bg-9-57-2012

Lazzari, P., Solidoro, C., Ibello, V., Salon, S., Teruzzi, A., Béranger, K., et al. (2012). Seasonal and inter-annual variability of plankton chlorophyll and primary production in the Mediterranean Sea: A modelling approach. *Biogeosciences*, *9*(1), 217–233. https://doi.org/10.5194/bg-9-217-2012

Liang, C., Amelung, W., Lehmann, J., & Kästner, M. (2019). Quantitative assessment of microbial necromass contribution to soil organic matter. *Global Change Biology*, *25*(11), 3578–3590. https://doi.org/10.1111/gcb.14781

Lüdmann, T., Wiggershaus, S., Betzler, C., & Hübscher, C. (2012). Southwest Mallorca Island: A cool-water carbonate margin dominated by drift deposition associated with giant mass wasting. *Marine Geology*, *307–310*, 73–87. https://doi.org/10.1016/j.margeo.2011.09.008

Magill, C. R., Ausín, B., Wenk, P., McIntyre, C., Skinner, L., Martínez-García, A., et al. (2018). Transient hydrodynamic effects influence organic carbon signatures in marine sediments. *Nature Communications*, *9*(1), 4690. https://doi.org/10.1038/s41467-018-06973-w

Martín, J., Puig, P., Masqué, P., Palanques, A., & Sánchez-Gómez, A. (2014). Impact of bottom trawling on deep-sea sediment properties along the flanks of a submarine canyon. *PLoS One*, *9*(8), e104536. https://doi.org/10.1371/journal.pone.0104536

Masqué, P., Fabres, J., Canals, M., Sanchez-Cabeza, J., Sanchez-Vidal, A., Cacho, I., et al. (2003). Accumulation rates of major constituents of hemipelagic sediments in the deep Alboran Sea: A centennial perspective of sedimentary dynamics. *Marine Geology*, *193*(3–4), 207–233. https://doi.org/10.1016/s0025-3227(02)00593-5

Masqué, P., Sanchez-Cabeza, J. A., Bruach, J. M., Palacios, E., & Canals, M. (2002). Balance and residence times of 210Pb and 210Po in surface waters of the northwestern Mediterranean Sea. *Continental Shelf Research*, *22*(15), 2127–2146. https://doi.org/10.1016/s0278-4343(02)00074-2

Mayer, L. M. (1994a). Relationships between mineral surfaces and organic carbon concentrations in soils and sediments. *Chemical Geology*, *114*(3–4), 347–363. https://doi.org/10.1016/0009-2541(94)90063-9

Mayer, L. M. (1994b). Surface area control of organic carbon accumulation in continental shelf sediments. *Geochimica et Cosmochimica Acta*, *58*(4), 1271–1284. https://doi.org/10.1016/0016-7037(94)90381-6

Mayot, N., D'Ortenzio, F., Taillandier, V., Prieur, L., de Fommervault, O. P., Claustre, H., et al. (2017). Physical and biogeochemical controls of the phytoplankton blooms in North Western Mediterranean Sea: A multiplatform approach over a complete annual cycle (2012–2013 DEWEX experiment). *Journal of Geophysical Research: Oceans*, *122*(12), 9999–10019. https://doi.org/10.1002/2016jc012052

McCallister, S. L., Bauer, J. E., Cherrier, J. E., & Ducklow, H. W. (2004). Assessing sources and ages of organic matter supporting river and estuarine bacterial production: A multiple-isotope (Δ¹⁴C, δ¹³C, and δ¹⁵N) approach. *Limnology & Oceanography*, *49*(5), 1687–1702. https://doi.org/10.4319/lo.2004.49.5.1687

Meyers, P. A. (1994). Preservation of elemental and isotopic source identification of sedimentary organic matter. *Chemical Geology*, *114*(3–4), 289–302. https://doi.org/10.1016/0009-2541(94)90059-0

Miralles, J., Radakovitch, O., & Aloisi, J. C. (2005). 210Pb sedimentation rates from the Northwestern Mediterranean margin. *Marine Geology*, *216*(3), 155–167. https://doi.org/10.1016/j.margeo.2005.02.020

Mollenhauer, G., Kienast, M., Lamy, F., Meggers, H., Schneider, R. R., Hayes, J. M., & Eglinton, T. I. C. P. A. (2005). *An evaluation of 14C age relationships between co-occurring foraminifera, alkenones, and total organic carbon in continental margin sediments* (p. PA1016). Paleoceanography.

O'Connell, S., Alonso, B., Kastens, K. A., Maldonado, A., Malinverno, A., Nelson, C. H., et al. (1985). Morphology and downslope sediment displacement in a deep-sea valley, the Valencia Valley (Northwestern Mediterranean). *Geo-Marine Letters*, *5*(3), 149–156. https://doi.org/10.1007/bf02281632

Ogrinc, N., Markovics, R., Kanduč, T., Walter, L. M., & Hamilton, S. K. (2008). Sources and transport of carbon and nitrogen in the River Sava watershed, a major tributary of the River Danube. *Applied Geochemistry*, *23*(12), 3685–3698. https://doi.org/10.1016/j.apgeochem.2008.09.003

Ohkouchi, N., Eglinton, T. I., Keigwin, L. D., & Hayes, J. M. (2002). Spatial and temporal offsets between proxy records in a sediment drift. *Science*, *298*(5596), 1224–1227. https://doi.org/10.1126/science.1075287

Ollivier, P., Hamelin, B., & Radakovitch, O. (2010). Seasonal variations of physical and chemical erosion: A three-year survey of the Rhone River (France). *Geochimica et Cosmochimica Acta*, *74*(3), 907–927. https://doi.org/10.1016/j.gca.2009.10.037

Palanques, A., Durrieu de Madron, X., Puig, P., Fabres, J., Guillén, J., Calafat, A., et al. (2006). Suspended sediment fluxes and transport processes in the Gulf of Lions submarine canyons. The role of storms and dense water cascading. *Marine Geology*, *234*(1–4), 43–61. https://doi.org/10.1016/j.margeo.2006.09.002

Palanques, A., Puig, P., Guillén, J., Demestre, M., & Martín, J. (2014). Effects of bottom trawling on the Ebro continental shelf sedimentary system (NW Mediterranean). *Continental Shelf Research*, *72*, 83–98. https://doi.org/10.1016/j.csr.2013.10.008

Paradis, S., Arjona-Camas, M., Goñi, M., Palanques, A., Masqué, P., & Puig, P. (2022). Contrasting particle fluxes and composition in a submarine canyon affected by natural sediment transport events and bottom trawling. *Frontiers in Marine Science*, *9*. Original Research. https://doi.org/10.3389/fmars.2022.1017052

Paradis, S., Goñi, M., Masqué, P., Durán, R., Arjona-Camas, M., Palanques, A., & Puig, P. (2021). Persistence of biogeochemical alterations of deep-sea sediments by bottom trawling. *Geophysical Research Letters*, *48*(2), e2020GL091279. https://doi.org/10.1029/2020gl091279

Paradis, S., Lo Iacono, C., Masqué, P., Puig, P., Palanques, A., & Russo, T. (2021). Evidence of large increases in sedimentation rates due to fish trawling in submarine canyons of the Gulf of Palermo (SW Mediterranean). *Marine Pollution Bulletin*, *172*, 112861. https://doi.org/10.1016/j.marpolbul.2021.112861

Paradis, S., Puig, P., Sanchez-Vidal, A., Masqué, P., Garcia-Orellana, J., Calafat, A., & Canals, M. (2018). Spatial distribution of sedimentation-rate increases in Blanes Canyon caused by technification of bottom trawling fleet. *Progress in Oceanography*, *169*, 241–252. https://doi.org/10.1016/j.pocean.2018.07.001

Pedrosa-Pàmies, R., Sanchez-Vidal, A., Calafat, A., Canals, M., & Durán, R. (2013). Impact of storm-induced remobilization on grain size distribution and organic carbon content in sediments from the Blanes Canyon area, NW Mediterranean Sea. *Progress in Oceanography*, *118*, 122–136. https://doi.org/10.1016/j.pocean.2013.07.023

Puig, P., Canals, M., Company, J. B., Martín, J., Amblas, D., Lastras, G., et al. (2012). Ploughing the deep sea floor. *Nature*, *489*(7415), 286–289. https://doi.org/10.1038/nature11410

Quirós-Collazos, L., Pedrosa-Pàmies, R., Sanchez-Vidal, A., Guillén, J., Duran, R., & Cabello, P. (2017). Distribution and sources of organic matter in size-fractionated nearshore sediments off the Barcelona city (NW Mediterranean). *Estuarine, Coastal and Shelf Science*, *189*, 267–280. https://doi.org/10.1016/j.ecss.2017.03.004

Rau, G. H., Takahashi, T., & Marais, D. J. D. (1989). Latitudinal variations in plankton δ¹³C: Implications for CO_2 and productivity in past oceans. *Nature*, *341*(6242), 516–518. https://doi.org/10.1038/341516a0

Relvas, P., Barton, E. D., Dubert, J., Oliveira, P. B., Peliz, Á., da Silva, J. C. B., & Santos, A. M. P. (2007). Physical oceanography of the western Iberia ecosystem: Latest views and challenges. *Progress in Oceanography*, *74*(2–3), 149–173. https://doi.org/10.1016/j.pocean.2007.04.021

Romero, E., Garnier, J., Billen, G., Peters, F., & Lassaletta, L. (2016). Water management practices exacerbate nitrogen retention in Mediterranean catchments. *Science of the Total Environment*, *573*, 420–432. https://doi.org/10.1016/j.scitotenv.2016.08.007

Sanchez-Cabeza, J., Masqué, P., & Ani-Ragolta, I. (1998). 210Pb and210Po analysis in sediments and soils by microwave acid digestion. *Journal of Radioanalytical and Nuclear Chemistry*, *227*(1–2), 19–22. https://doi.org/10.1007/bf02386425

Sanchez-Vidal, A., Pasqual, C., Kerhervé, P., Heussner, S., Calafat, A., Palanques, A., et al. (2009). Across margin export of organic matter by cascading events traced by stable isotopes, northwestern Mediterranean Sea. *Limnology & Oceanography*, *54*(5), 1488–1500. https://doi.org/10.4319/lo.2009.54.5.1488

Sarhan, T., García Lafuente, J., Vargas, M., Vargas, J. M., & Plaza, F. (2000). Upwelling mechanisms in the northwestern Alboran Sea. *Journal of Marine Systems*, *23*(4), 317–331. https://doi.org/10.1016/s0924-7963(99)00068-8

Siokou-Frangou, I., Christaki, U., Mazzocchi, M. G., Montresor, M., Ribera d'Alcalá, M., Vaqué, D., & Zingone, A. (2010). Plankton in the open Mediterranean Sea: A review. *Biogeosciences*, *7*(5), 1543–1586. https://doi.org/10.5194/bg-7-1543-2010

Soria-Jáuregui, Á., Jiménez-Cantizano, F., & Antón, L. (2019). Geomorphic and tectonic implications of the endorheic to exorheic transition of the Ebro River system in northeast Iberia. *Quaternary Research*, *91*(2), 472–492. https://doi.org/10.1017/qua.2018.87

Stabholz, M., Durrieu de Madron, X., Canals, M., Khripounoff, A., Taupier-Letage, I., Testor, P., et al. (2013). Impact of open-ocean convection on particle fluxes and sediment dynamics in the deep margin of the Gulf of Lions. *Biogeosciences*, *10*(2), 1097–1116. https://doi.org/10.5194/bg-10-1097-2013

Struglia, M. V., Mariotti, A., & Filograsso, A. (2004). River discharge into the Mediterranean Sea: Climatology and aspects of the observed variability. *Journal of Climate*, *17*(24), 4740–4751. https://doi.org/10.1175/jcli-3225.1

Stuiver, M., & Polach, H. A. (1977). Discussion reporting of 14C data. *Radiocarbon*, *19*(3), 355–363. https://doi.org/10.1017/s0033822200003672

Tesi, T., Goñi, M. A., Langone, L., Puig, P., Canals, M., Nittrouer, C. A., et al. (2010). Reexposure and advection of 14C-depleted organic carbon from old deposits at the upper continental slope. *Global Biogeochemical Cycles*, *24*(4), GB4002. https://doi.org/10.1029/2009gb003745

Tesi, T., Miserocchi, S., Goñi, M. A., Langone, L., Boldrin, A., & Turchetto, M. (2007). Organic matter origin and distribution in suspended particulate materials and surficial sediments from the western Adriatic Sea (Italy). *Estuarine, Coastal and Shelf Science*, *73*(3–4), 431–446. https://doi.org/10.1016/j.ecss.2007.02.008

Ulses, C., Estournel, C., Puig, P., Durrieu de Madron, X., & Marsaleix, P. (2008). Dense shelf water cascading in the northwestern Mediterranean during the cold winter 2005: Quantification of the export through the Gulf of Lion and the Catalan margin. *Geophysical Research Letters*, *35*(7), L07610. https://doi.org/10.1029/2008gl033257

Verwega, M. T., Somes, C. J., Schartau, M., Tuerena, R. E., Lorrain, A., Oschlies, A., & Slawig, T. (2021). Description of a global marine particulate organic carbon-13 isotope data set. *Earth System Science Data*, *13*(10), 4861–4880. https://doi.org/10.5194/essd-13-4861-2021

Wacker, L., Lippold, J., Molnár, M., & Schulz, H. (2013). Towards radiocarbon dating of single foraminifera with a gas ion source. *Nuclear Instruments and Methods in Physics Research Section B: Beam Interactions with Materials and Atoms*, *294*, 307–310. https://doi.org/10.1016/j.nimb.2012.08.038

Wada, E., & Hattori, A. (1991). Nitrogen in the Sea: Forms, abundances, and rate processes.

Welte, C., Hendriks, L., Wacker, L., Haghipour, N., Eglinton, T. I., Günther, D., & Synal, H.-A. (2018). Towards the limits: Analysis of microscale ^{14}C samples using EA-AMS. *Nuclear Instruments and Methods in Physics Research Section B: Beam Interactions with Materials and Atoms*, *437*, 66–74. https://doi.org/10.1016/j.nimb.2018.09.046

Würtz, M. (2012). Mediterranean submarine canyons: Ecology and governance.

Zonneveld, K. A. F., Versteegh, G. J. M., Kasten, S., Eglinton, T. I., Emeis, K. C., Huguet, C., et al. (2010). Selective preservation of organic matter in marine environments; processes and impact on the sedimentary record. *Biogeosciences*, *7*(2), 483–511. https://doi.org/10.5194/bg-7-483-2010

Zuo, Z., Eisma, D., Gieles, R., & Beks, J. (1997). Accumulation rates and sediment deposition in the northwestern Mediterranean. *Deep Sea Research Part II: Topical Studies in Oceanography*, *44*(3–4), 597–609. https://doi.org/10.1016/s0967-0645(96)00083-5